University of Sadat City
Environmental Studies and Research Institute
The4Th International Conference
Environmental for Studies and Research Smart Sustainable Environment

Journal of Environmental Studies and Researches (2017), 7(2-D): 955- 969

ASSESSMENT VULNERABILITY OF THE LOW LAND ZONE SOUTH EAST OF ALEXANDRIA, EGYPT

El-Hattab M.[(1)], H. El-Askary[(2)], and M. El-Raey[(3)]

(1) Environmental Studies and Research Institute, University of Sadat City, Egypt. **mmelhattab@Gmail.com**
(2) Chapman University, Orange, CA, United States. **elaskary@chapman.edu**
(3) Institute of Graduated Studies and Research (IGSR) – Alexandria University, Egypt. **Melraey01@link.net**

ABSTRACT:

Coastal areas are dynamic and complex multi-function environmental systems; it characterizes by significant ecological and natural values in addition to excellent habitat and biological diversity.

Sea level rise (SLR) and extreme water levels are the most important signs of the impacts of climate change causing major threats to human beings around the world particularly in fragile zones like Deltas and low-lying coastal areas. The potential effects increased when populations and their related economic activities highly concentrated along the coastal areas (M. M. El-Hattab, 2015).

A study of the geomorphology of large coastal area (that historically covered by both Lake Mareotis and Abu Qir Lagoon), including East of Alexandria City, Abu Qir city, Lake Idku, Kafr El Dauwar city, and the estuary of the river Nile (Rosetta branch), has been carried out for assessment of the vulnerability of the area to the impact of sea level rise.

Recent observations of the mean sea level all over the world lead to a low rise of 1.2 mm/yr during the last hundred years (El-Raey, 1990). The relationship between rising sea level and the rate of shoreline erosion has formulated. A close correlation between sea level rise and shoreline retreat has checked for the Egyptian coast (Frihy, 1991). Seasonal and annual variation in sea level parameters (high-high water level, low-low water level, mean water level, mean high water level, and mean low water level) were studied (Manohar, 1981), (Hamid and El Gindy, 1988).

Landsat Enhanced Thematic Mapper (ETM+) data were used to identify and delineate the geomorphological features, and a supervised classification technique was executed to extract an accurate and detailed land cover map. A geographic information system (GIS) has built including layers of land cover and topography (that created by interpolation all the available height information). Analysis of GIS data has been carried out to assess the vulnerability of various land cover classes to the possible impact of sea level rise.

Additionally, existing geological and topographical maps of the areas used as added information for elevation data, and to relate the classification results to the relief of the study area to build a Geographic Information System capable of identifying vulnerable areas to the sea level rise.

Results indicate that most of the vulnerable areas are vegetated land (over 50%), followed by bare soil (over 17%), and the high-density urban areas constitute about 5-6%. The vegetation below sea level that represents a significant percentage of the distribution of total vegetation cover indicates that severe economic losses may incur if no action for protection is taken.

Future protection measures against impacts of sea level rise and the risk of large storms and salt water intrusion are highly recommended. These include landfilling of weak tunnels, implementation of sewerage systems, upgrading of land drainage systems and raising of awareness of stakeholders and decision makers

KEYWORDS: *Geomorphology – Remote Sensing – Global Warming - Nile delta - GIS - Vulnerability to climate change.*

1. INTRODUCTION

Since the beginning of this century, the Nile Delta coast showed large erosional changes (Smith and Abdel-Kader, 1988); (Fanos et al., 1991); and (Frihy et., al 1994). According to coastal processes, the beaches have some morphologic changes (Scott, 1954); (Davis and Fox, 1972); (El Askary and Frihy, 1986), (M. El-Hattab, 2016).

The impact of an atmospheric warming and sea levels 30-70 cm higher than at present on the coastal lowlands of the Nile Delta during the next 50 to 100 years. It will depend not only on the degree of population and economic activities but also on the degree of coastal development during the next 2-3 decades (Sestini, 1991). This paper presents the work carried out to assess to what extent geological and geomorphological features could affect the vulnerability of the coastal areas to sea level rise. The sediment distribution on the continental shelf of the Nile Delta has been described well by some authors (EL Wakeel et al., 1974); (Summerhayes and Mark, 1976); and (El-Raey et., al 1995). These studies agree in showing sands near shore and on the outer shelf of the Delta, and muds on the Rosetta and Damietta cones.

Detailed information on surface morphology or information about surface land cover properties of coastal areas is important issues for proper assessment of impacts of sea level rise and adaptation. Unfortunately, limited detailed information is usually available, where field data collected.

Historically, the site to the east south covered by an old lake called Abu Qir Lagoon. The building of Mohamed Ali Wall separated the lake from Abu Qir Bay, and the Lake later dried with some parts of adjacent Lake Maryut. The dry areas cultivated for some time and later many places were urbanized and inhabited. Most of the population and decision makers still do not realize that they located below sea level. Figure (1) represents an old map of the region which indicates that most of the area located below the sea level and in fact, Mohamed Ali Wall represents the only protection against the flow of the bay into this low-land area.

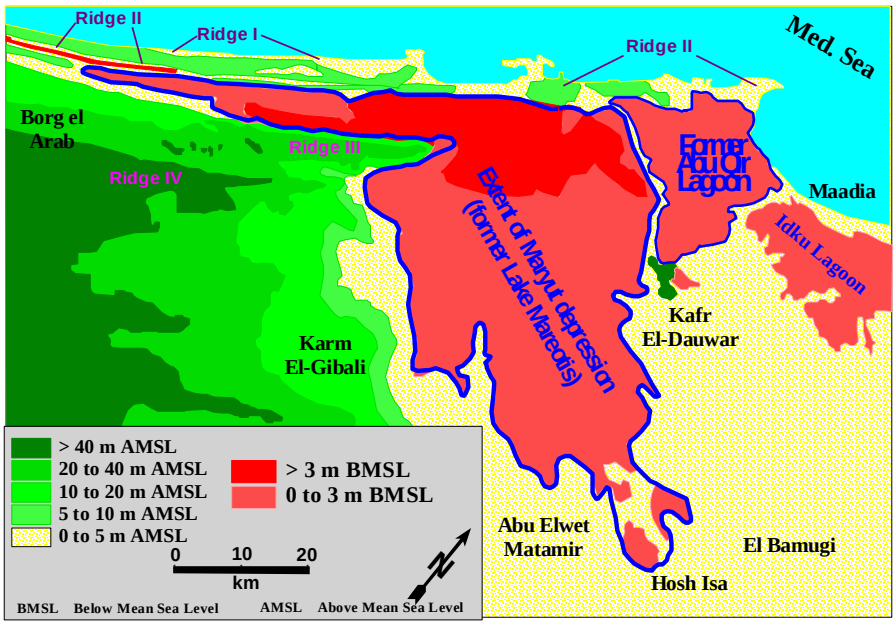

Figure (1): Low elevation land to the south-east of Alexandria City. It indicates the Old Abu Qir Lagoon and Lake Maryut. (Primary Source of data: US Defense Mapping Agency 1961, 1973, 1975, 1977)

It realized that these areas are not only to impacted by potential effects of climate changes and sea level rise, but it is also under the severe risk of sudden inundation by extreme events of marine storms or damages to Mohamed Ali sea wall. The primary objective of this study is to identify and assess land uses and potential losses of the region and to explore options for risk reduction and adaptation.

Satellite remote sensing is potentially powerful means of monitoring land-use change at high temporal resolution and lower costs than those associated with the use of traditional methods. (Adeniyi, 1985). All available approaches for change detection were checked to use the best available one (Susan et al., 1990), (Fung and LeDrew, 1987), (Howarth and Wickmore, 1981), (Nelson, 1983), (Robinove et al., 1983).

Image processing classification results show that significant detailed information can extracted from the satellite data, the information did not include only the geomorphology, but it includes land cover and land uses of the study area.

2. AVAILABLE DATA And MERGING

Two recent LANDSAT ETM+ satellite images are acquired and used to cover the study area. The ETM+ images characterized by spatial resolution of 28 meters (multispectral bands). By using advanced image processing algorithms, the panchromatic band (spatial resolution of 14.25 meters) of the image that uses the visible range of light merged with other multispectral bands. According to merging process, the image spatial and spectral resolutions improved. The final characteristics of the satellite image (that will use as the source of various land cover features)

will be six spectral bands of 14.25-meter spatial resolution. The resolution achieved could be considered reasonable for the purposes and goals of this study.

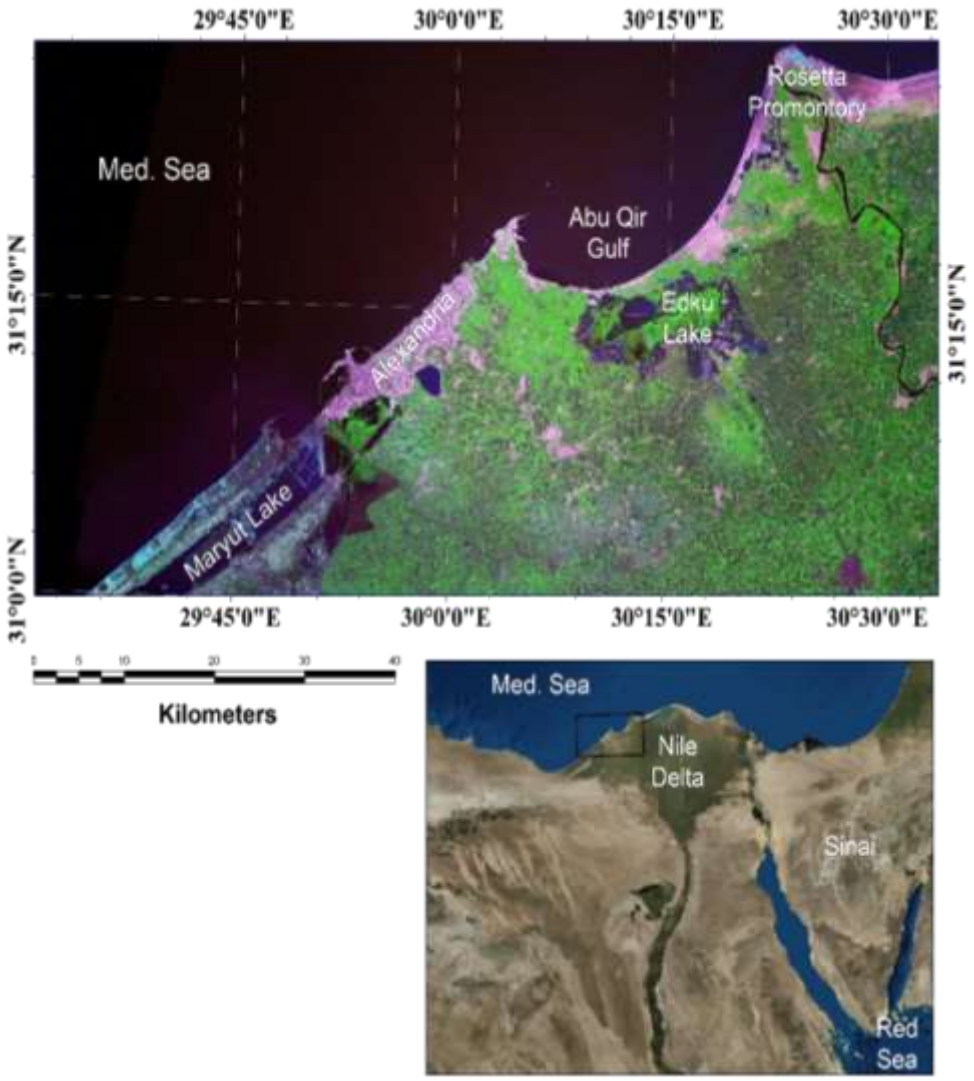

Figure (2): The site location and details of the area under consideration

3. SATELLITE IMAGE PROCESSING

Several steps were carried out to prepare the satellite image to become a proper reference for GIS layers (GIS-ready). Those measures include:

1. Adjusting the image that covers whole study area.
2. Image registration
3. Image rectification
4. Spatial resolution merge
5. Image processing (Filtering, Smoothing, etc.)

First; two recent LANDSAT/ ETM+ images were mosaicked to cover the study area, as the study area is larger than one LANDSAT scene. After acquiring the image that covers the whole are, digital image processing techniques were carried out; it includes preprocessing, enhancement, and classification.

3.1. Image Pre-Processing:

The pre-processing techniques refer to the initial processing of the raw data to calibrate the image radiometry, correct geometric distortion and remove noise. The image was then geometrically corrected using fixed ground control points to ensure that the image has the proper geometric characteristics. Then it was rectified using a large number of ground control points and registered using WGS84 as a reference datum and ellipsoid, UTM as map projection using +36 zone number. Figure (3) illustrates the satellite image after pre-processing.

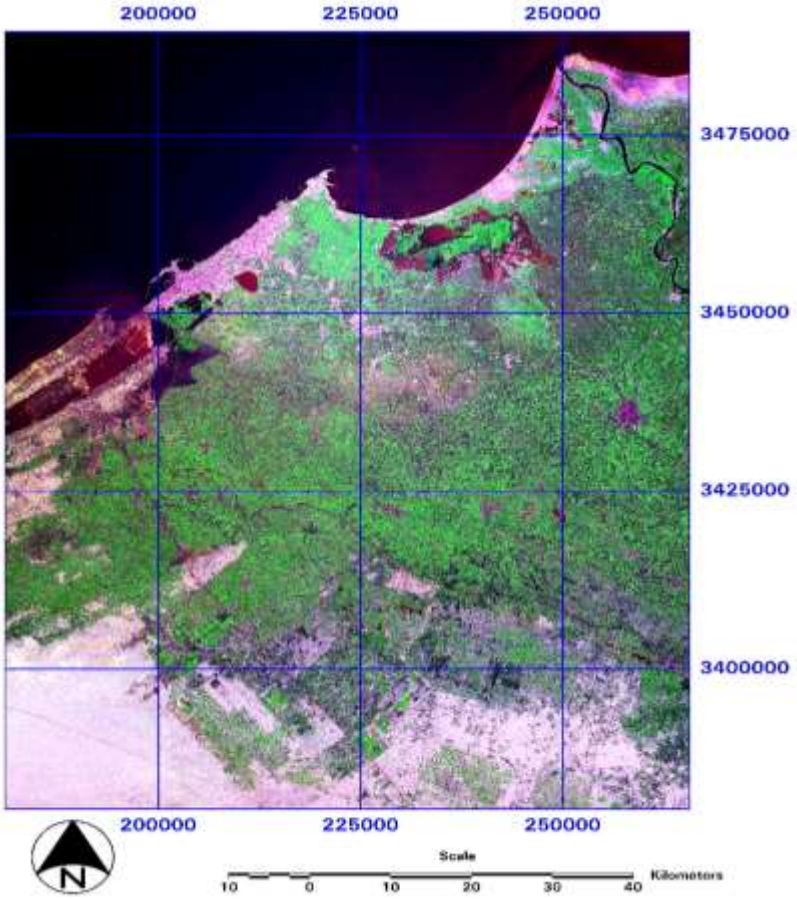

Figure (3): LANDSAT ETM+ Image of the Study area

4. LAND COVERS MAP PRODUCTION:

The production of the land cover map from the pre-processed image was achieved using high accuracy classification techniques.

4.1. Classification of satellite image:

The satellite image was hybrid classified, which consists of two main steps, unsupervised classification followed by supervised classification.

4.1.1. Unsupervised Classification:

The unsupervised classification carries out natural clustering of all pixels of the image into the main clusters (land cover classes) of the area. In spite of being of relatively low accuracy, it used to reduce time and effort.

By using accuracy threshold level of 99.9%, the number of clusters obtained from this step is 100 different clusters with its 100 spectral signatures.

4.1.2. Supervised Classification:

This step is the second phase of the process, which began with assessing all the 100 spectral signatures (produced through unsupervised classification) and comparing it to some spectral signatures collected from field surveys. According to the detailed study of the spectral signatures, all similar signatures combined. The maximum likelihood classification (MLC) algorithm used in the classification process. Only six spectral signatures were found to be entirely separable (having a unique signature and digital number range value), i.e. the final classified image has a six different classes. The six land cover classes in the supervised classification image (Figure 4) identified as:

1. Water Bodies (including all bodies such as River Nile, Sea, Lakes,etc.)
2. Wet Vegetation (mainly the brackish water vegetation and some inland vegetation such as Rice)
3. Vegetation (all types of plants and fruits as well)
4. Plowed Fields (agricultural lands prepared for plantation and has small percentages of natural vegetation)
5. Bare Soil (includes all areas with no vegetation cover and no land uses)
6. Urban (includes fabricated high-density urban centres, medium density urban areas, low-density cities, slums and rural areas).

4.1.3. Accuracy Assessment:

The supervised classification accuracy percentage calculated by measuring the percentage of correctly classified pixels according to ground truth data; it was found to be 97.8% which was acceptable.

5. INTEGRATING SATELLITE And GEOGRAPHIC INFORMATION SYSTEMS:

Increasing interest show in the combined use of remotely sensed images and GIS based data sets for environmental applications. There is a great need for raster processing facilities because environmental parameters are continuous and have no firm boundaries. Data stored in a GIS needs to converted into raster format to be integrated into the image processing chain, on the other hand, integration of remotely sensed data into a vector system requires more effort but can be achieved by using an image as a backdrop for vector editing and on-screen digitizing.

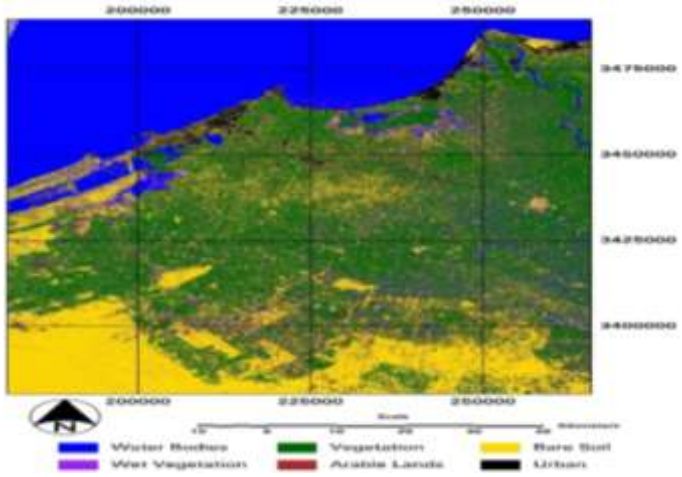

Figure (4): Supervised classification image

All data placed within the GIS structure with all its cross-relations. The classified image converted into a land cover map within the geographic information system, the produced image was first smoothed using "Low Pass" filter to make clusters polygon's boundaries smooth. The second step is to convert the smoothed classified image into a particular format the GIS system could accept. The file converted into "LAN" format, then into "GRID" format, using ERDAS IMAGINE software.

The next step of producing the land cover map is to import the supervised classification image into the system that has been done using ARC GIS software. The image imported into the GIS as Grid file, and then it was saved as a "SHAPE" file typical of GIS layers. Finally, the "Querry Builder" module in the ARCGIS system was used to reclassify the GIS layer into six separate GIS layers each represents one of the land cover classes, as in Figure (5). All the GIS layers then overlayed in one GIS layer representing the land cover map, as in Figure (6).

6. ELEVATION MAP:

The elevation map is one of the primary GIS layers in the study, as it determines zones that could affect by sea level rise and zones that lie under danger of flooding by water. The elevation layer consumes the largest time in comparing with other GIS layers; it is produced in several steps as follows:

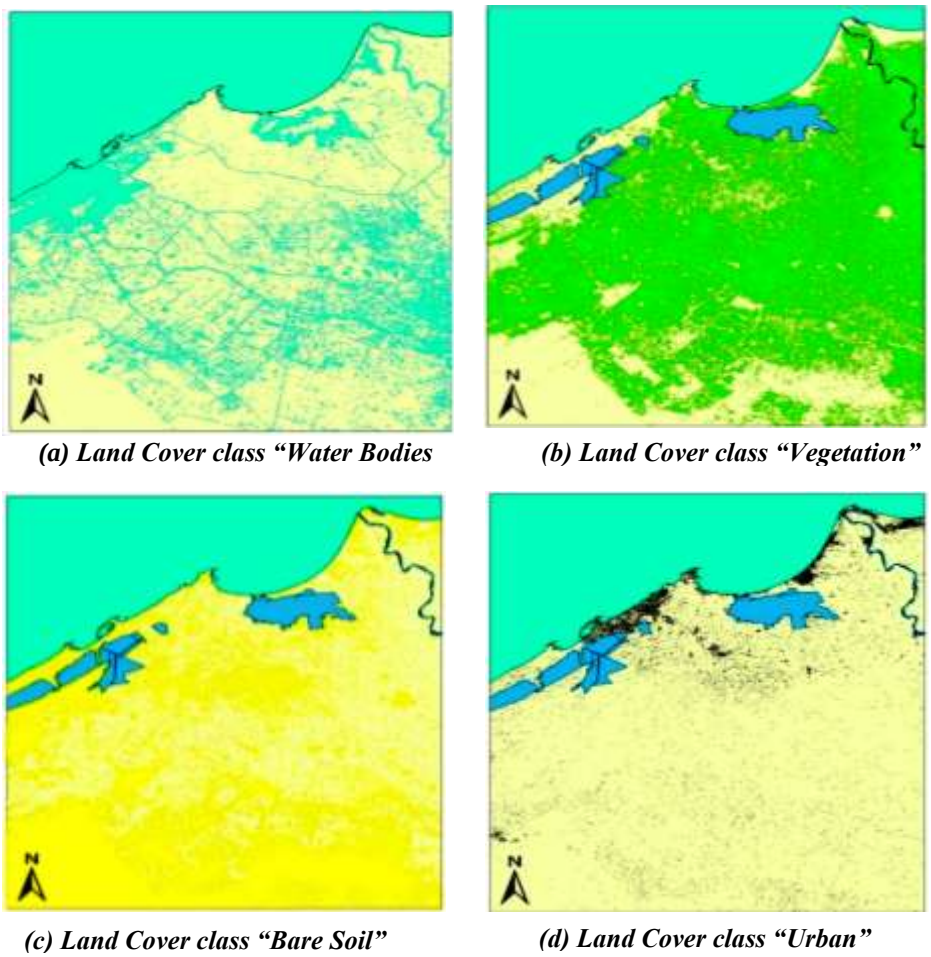

(a) Land Cover class "Water Bodies *(b) Land Cover class "Vegetation"*

(c) Land Cover class "Bare Soil" *(d) Land Cover class "Urban"*

Figure (5): Some of the GIS layers

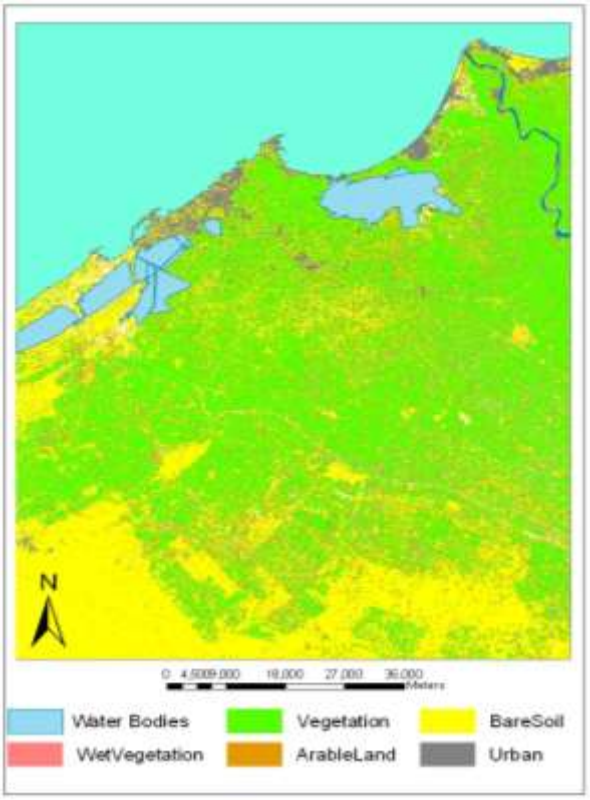

Figure (6): Land Cover Map obtained from Classification of Satellite Image

6.1. Elevation data collection:

The available elevation data have two types (format), they either points or lines. The point data layer edited and verified; Figure 7.

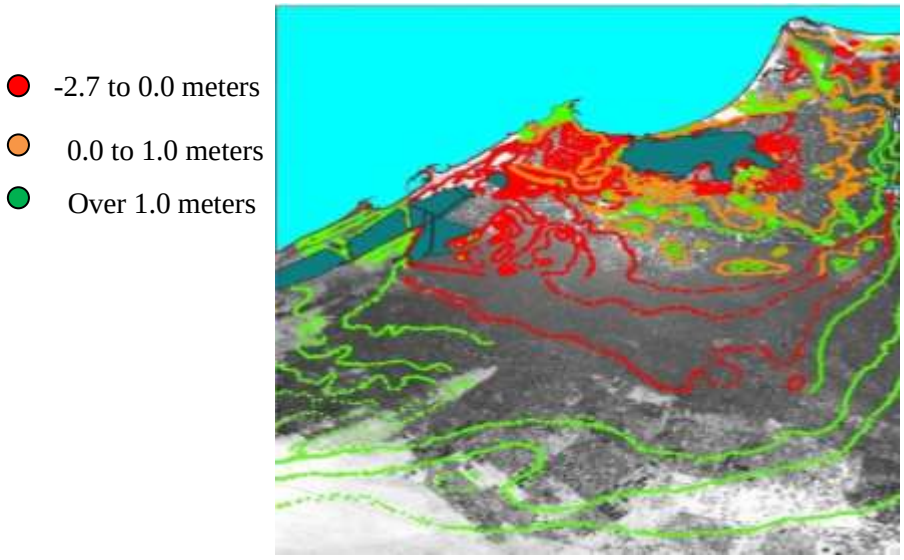

Figure (7): Point elevation data

The other type of the elevation data is the contour lines maps, which is converted into elevation points and then overlaid on the previously prepared elevation point data layer. Figure (8) illustrates the two types of elevation data after overlaying.

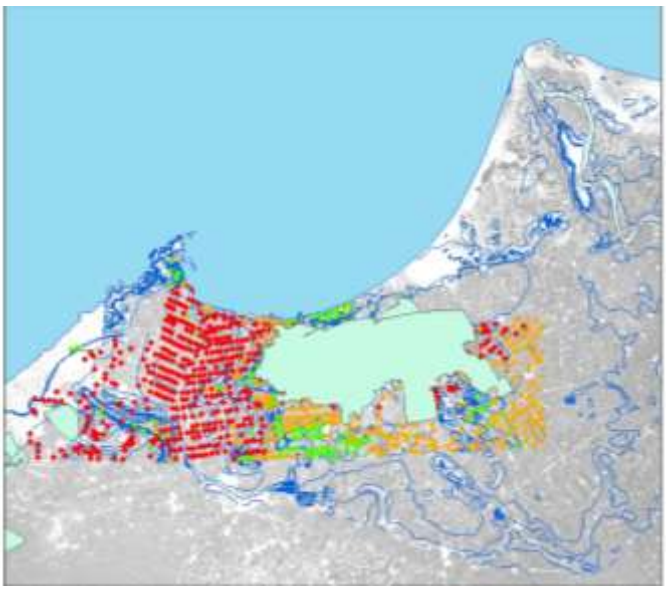

Figure (8): Overlaid elevation data

Finally, field surveys used in areas not covered by GPS to meet gaps in elevation points data. So, all elevation points interpolated and converted to raster form. "Spline" model was used to interpolate raster GIS layer and cover the elevation range from -2.7 meters to more than 41 meters, increasing interval of 0.7 meters. The total number of height values produced is 65 values. To make the elevation map usable, all the generated 65 values were averaged into 22 values. Figure (9) represents the interpolated averaged elevation raster map.

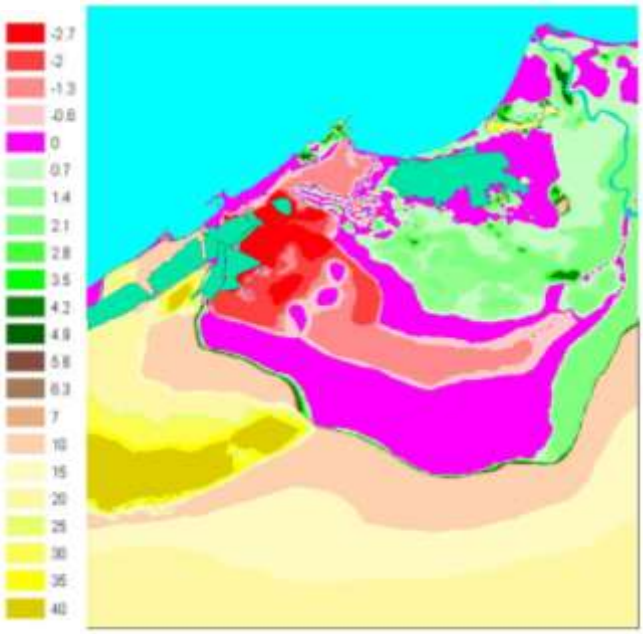

Figure (9): Produced Interpolation Averaged Elevation map

7. OVERLAYING LAND COVER MAP And ELEVATION MAP:

This step is one of the most important stages in the study, it helps in zoning different land cover classes according to their elevation, thus identify areas located in the high-risk region. Figure 10, illustrates the overlaid map of both elevation and land cover maps. That step followed by producing a database of the overlaying resulting map, then converted into Excel format so as to analyze each elevation.

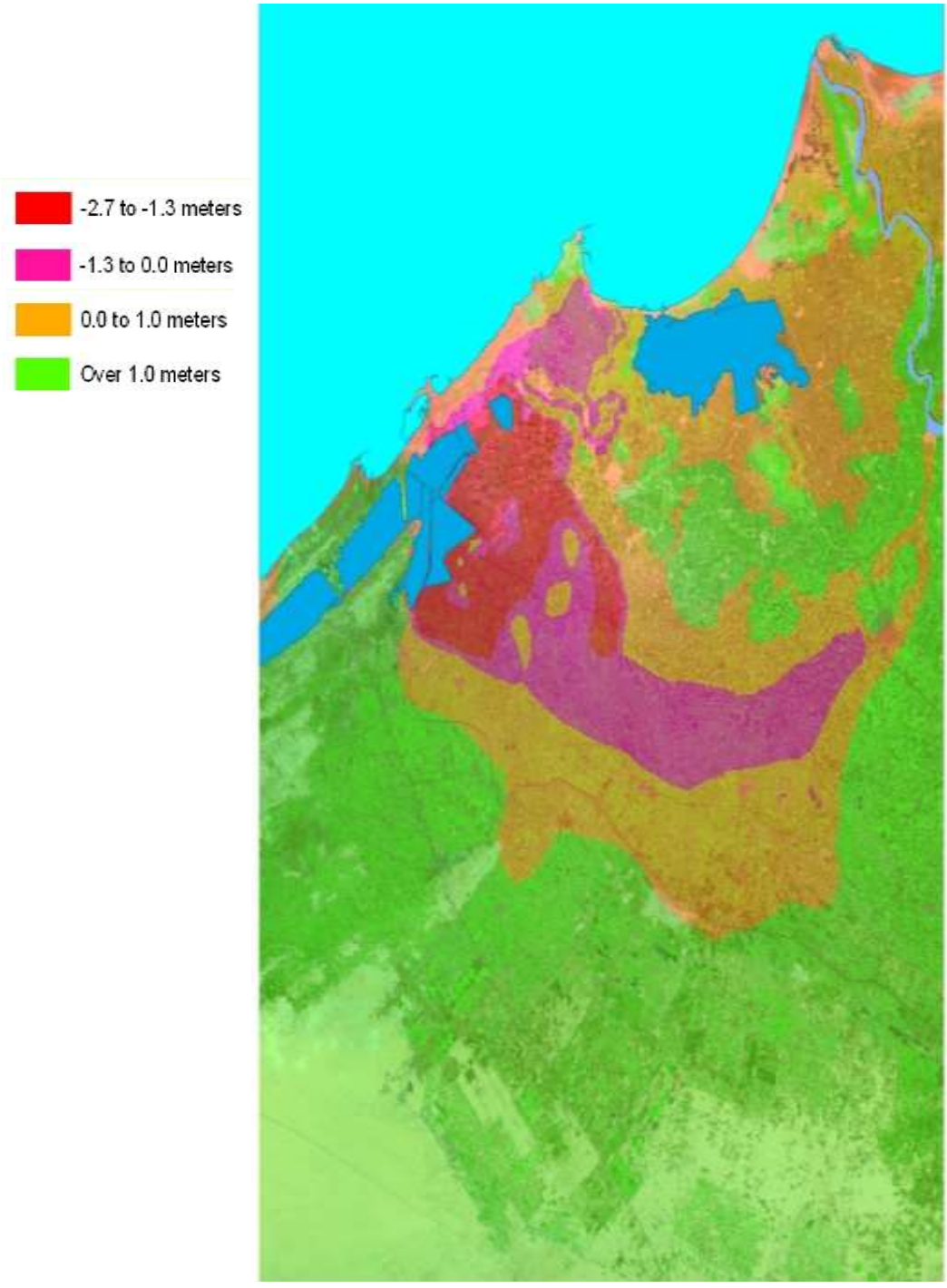

Figure (10): Overlaid elevation and land cover maps.

Table (1): Percentage of land covers for each elevation value

Average Elevation	Land Cover Percentage					
	Water Bodies	Wet Vegetation	Vegetation	Arable Lands	Bare Soil	Urban
-2.7	10.45%	4.21%	52.57%	5.41%	19.16%	8.20%
-2	1.77%	1.91%	66.68%	5.08%	20.37%	4.18%
-1.3	2.11%	16.52%	57.47%	4.83%	15.87%	3.20%
-0.6	8.35%	14.57%	52.29%	4.55%	14.67%	5.58%
0	73.78%	3.02%	4.90%	1.53%	3.89%	12.88%
0.1	71.29%	8.17%	6.75%	0.71%	1.79%	11.30%
0.8	0.53%	5.43%	65.33%	5.85%	15.63%	7.23%
1.5	0.20%	2.29%	39.25%	45.19%	8.94%	4.14%
2.2	0.10%	3.88%	43.97%	38.02%	10.12%	3.91%
2.9	0.46%	4.07%	60.40%	10.84%	21.74%	2.49%
3.6	0.11%	0.92%	48.23%	33.17%	16.37%	1.20%
4.3	0.08%	0.64%	41.06%	5.97%	49.27%	2.99%
5	0.28%	2.01%	37.23%	11.30%	14.71%	34.47%
5.7	0.30%	3.93%	62.77%	4.28%	18.67%	10.05%
6.4	0.17%	2.04%	49.11%	3.99%	16.14%	28.55%
7.1	0.15%	2.38%	48.58%	7.97%	17.38%	23.55%
7.8	0.12%	0.05%	30.98%	9.33%	16.24%	43.28%
8.5	0.14%	0.16%	47.53%	4.24%	17.65%	30.29%
9.2	0.24%	0.54%	63.82%	5.76%	24.21%	5.43%
9.9	0.31%	0.45%	8.37%	6.94%	79.41%	4.53%
10.6	0.10%	0.53%	56.58%	7.53%	29.99%	5.27%
11.3	0.13%	0.19%	9.66%	11.13%	76.98%	1.91%
12	0.23%	0.17%	24.67%	7.80%	65.92%	1.22%
12 to 20	0.00%	0.03%	16.83%	9.50%	73.63%	0.02%
20 to 30	0.00%	0.01%	15.95%	2.81%	78.44%	2.80%
30 to 40	0.03%	0.12%	62.46%	10.17%	25.95%	1.26%
more 40	0.02%	0.18%	67.90%	7.50%	23.25%	1.15%

Table(1) illustrates various land cover classes in each elevation interval. It is clear that there are large differences in percentage values in each height range. To show the relative proportions of different land cover classes over the various height ranges, a series of charts plotted for that purpose. From these graphs, all the data needed to understand the interaction between different land cover types and its elevation could be identified. Also, the status of each land cover type and its vulnerability to the expected sea level rise could identify.

Next figures represent those charts that illustrate the distribution of each different land cover over the various elevation levels.

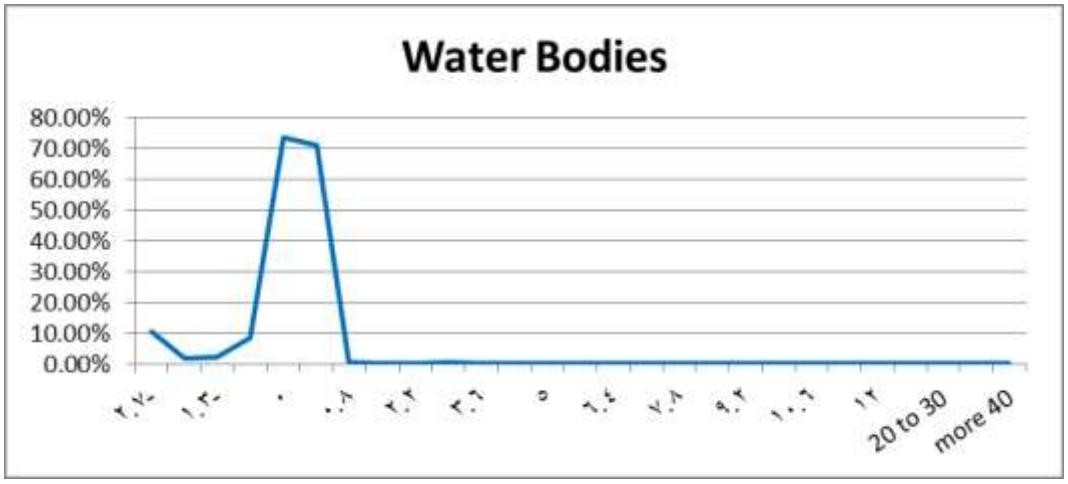

Figure (11): Percentage of "Water Bodies" land cover over the different average height values

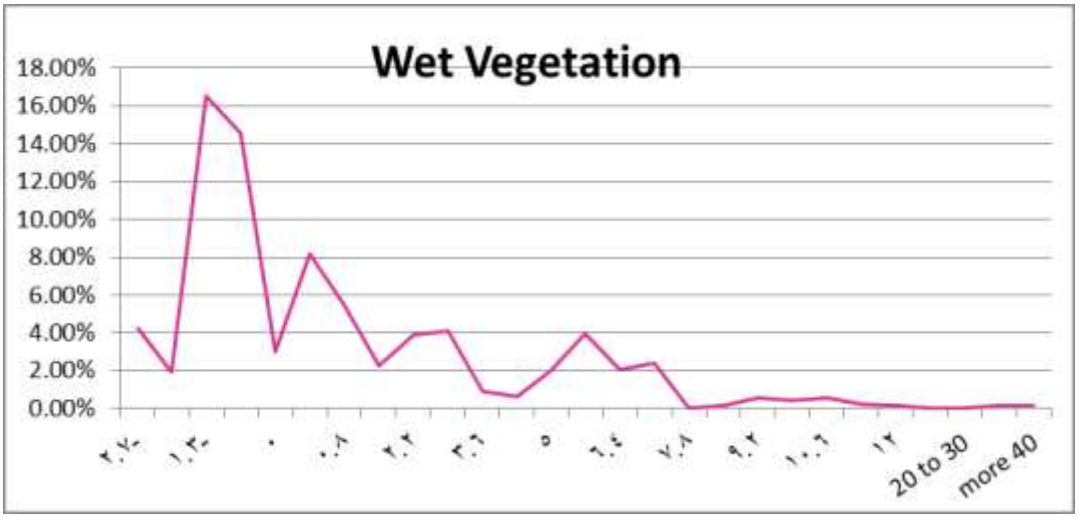

Figure (12): Percentage of "Wet Vegetation" land cover over the different average height values

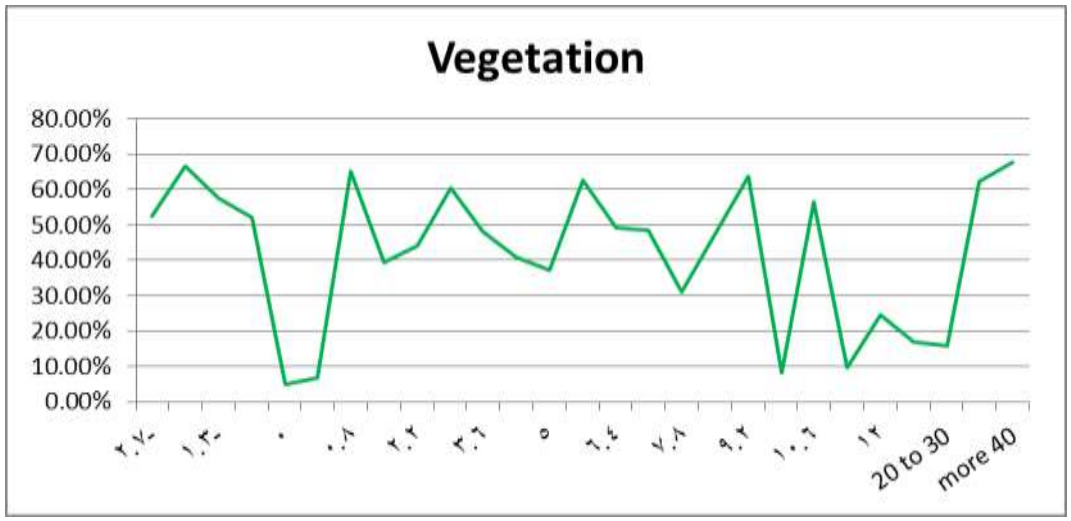

Figure (13): Percentage of "Vegetation" land cover over the various average elevation values

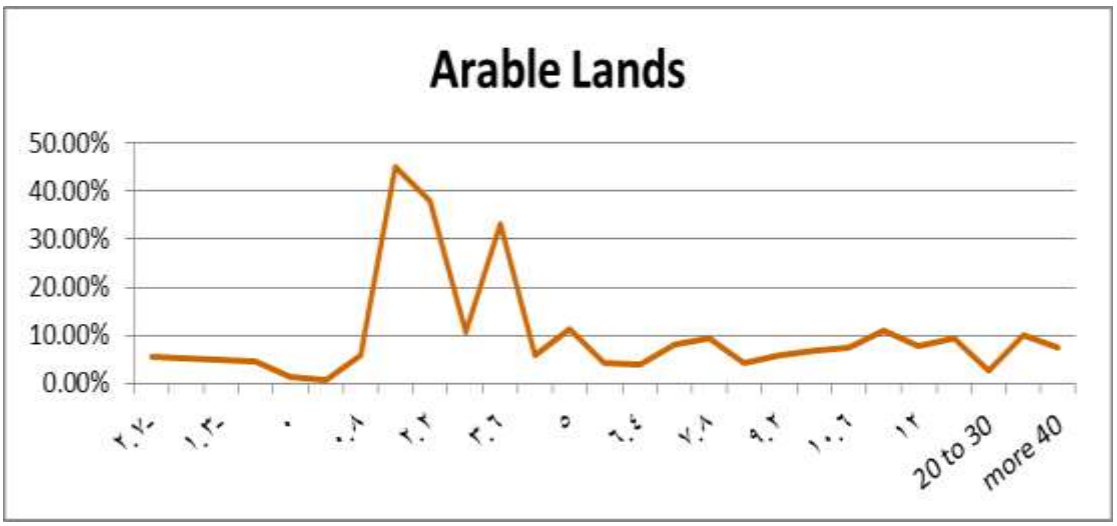

Figure (14): Percentage of "Arable Lands" land cover over the different average height values

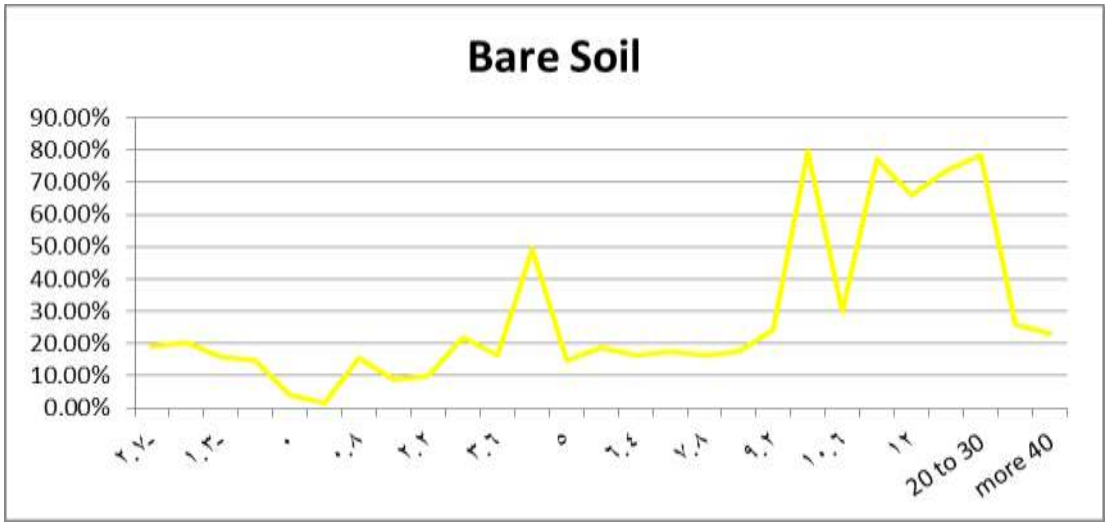

Figure (15): Percentage of "Bare Soil" land cover over the various average elevation values

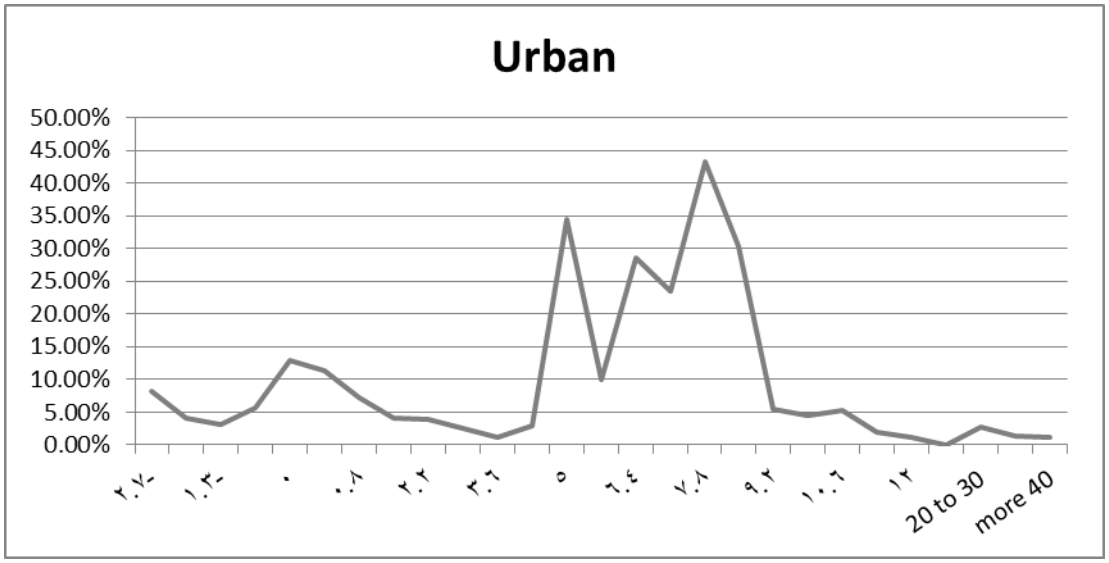

Figure (16): Percentage of "Urban" land cover over the different average height values

According to the previously illustrated diagrams, it well realized that:

(1) Most of the activities in the region lie at low elevation despite the availability of barren land on safe, high elevation areas.
(2) Physical enforcement of Mohamed Ali Seawall is a necessary prerequisite for any adaptation policy or measures in the region.
(3) The majority of the urban population is located at a relatively safe elevation intervals so that the cost of adaptation measures will not involve dislocation of the majority of inhabitants.

7. CONCLUSIONS And DISCUSSIONS

Historically, the area was known to be the site of the old Abu Qir Lagoon, which connected to Lake Maryout. At the beginning of 19th century, the farmers of the areas at the southern margins of the Maryout Lake complain about flooding their farms by the Lake's waters especially during Winter seasons. Thus Mohamed Ali (the Governor of Egypt that time) has established of Mohamed Ali Wall to the north of Abu Qir Lagoon that blocks the bay water from reaching these water bodies. As this wall still stands for a recent time, the dry land south of it used for agriculture at the beginning, and then it was later urbanized without actually realizing that it located below the level of sea water.

Later, it well recognized that the low elevation area is highly vulnerable to potential impacts of salt water intrusion and that it is subject to high risks of salt water intrusion. It was important to identify and assess land use distribution and its relationship to topography and hopefully to work out a way to minimize potential impacts on these lowland areas

This work uses remote sensing and GIS techniques to identify and assess the distribution of the land use over the lowland areas (in addition to the adjacent highland area). Results indicate that in areas with elevation average 2.7 meters below mean sea level the most dominant land cover is "vegetation" (about 52% of the total area). It followed by "bare soil," "urban," and "arable lands" that constitute 19%, 8%, and 5%, respectively. In areas with elevation average 2.0 meters, below mean sea level the most dominant land cover is "vegetation" (about 66% of the total area), followed by "bare soil," "arable lands," and "urban" that represent 20%, 5%, and 4% respectively. Also for other lowland areas, the vegetation land cover class is the most dominant class.

Those results indicate that the area has an environmental problem and needs urgent plans for protection, risk reduction and adaptation measures such as:

(1) Monitoring of water logged areas, salt-effected lands, and slum areas to establish a combating plan.
(2) Development of a socioeconomic awareness program for stakeholders and decision makers
(3) Development of agricultural and municipal infrastructure and waste water treatment facilities
(4) Development of an action plan to be followed for upgrading the region making use of the extensive touristic resources of the area.

ACKNOWLEDGMENT

The authors acknowledge the support of CIRCE project (Climate Change and Impact Research the Mediterranean Environment) for carrying out this work. The support of the National Authority for Remote Sensing and Space Sciences also appreciated.

REFERENCES

- **Adeniyi, P.O. 1985**, Digital analysis of multi-temporal Landsat data for land use/land cover classifications in a semi-arid area in Nigeria, Photogrammetric Engineering and Remote Sensing, Vol. 51, No. 11, pp. 1761-1774.
- **Davis, R. A., and Fox, W. T., 1972**. Coastal processes and nearshore sand bars, J. Sediment. Petrol., Vol. 42, pp. 401-412.
- **El Askary, M. A., and Frihy, O. E., 1986**. Depositional phases of Rosetta and Damietta promontories on the Nile Delta coast, J. Afr. Earth Sci., Vol. 5, pp. 627-633.
- **El Raey, M., 1990.** Responses to the Impacts of Greenhouse-Induced Sea Level Rise on Egypt, Report to the Intergovernmental Panel on Climatic Change, from the Miami Conference on Adaptive Responses to Sea Level Rise and Other Impacts of Global Climatic Change, Vol. 2, pp. 225-233.
- **EL Wakeel, S. K., Abdou, H. F. and Mohamed, M. A., 1974**. Texture and distribution of recent marine sediments of the continental shelf of the Nile Delta. Jour. Geol. Soc. Iraq, Vol. 7, pp. 15- 34.
- **El-Raey, M.; S.M., Nasr; M.M. El-Hattab and O.E., Frihy, 1995**; Change detection of Rosetta promontory over the last forty years. International Journal of Remote Sensing, Vol. 16, No. 5, pp. 825-834.
- **Fanos, A. M., Frihy, O. E., Khafagy, A. A., and Komar, P. D., 1991.** Processes of shoreline changes along the Nile Delta coast of Egypt, Proceeding of a specially conference on quantitative approaches to coastal sediment processes, Coastal Sediments, Vol. 2, pp. 1547-1557.
- **Frihy, O. E., 1991.** Sea level rise and shoreline retreat of the Nile Delta promontories, Egypt, Natural Hazards, Vol. 2, pp. 65- 81.
- **Frihy, O.; S.M., Nasr; M.M., El-Hattab and M. El Raey, 1994**. Remote sensing of beach erosion along the Rosetta promontory, Northwestern Nile Delta, Egypt. International Journal of Remote Sensing, Vol. 15, No. 8, pp. 1649-1660.
- **Fung T. and E. LeDrew, 1987**. Application of principal components analysis to change detection, Photogrammetric Engineering and Remote Sensing, vol. 53, No. 12, pp. 1649-1658.
- **Hamid, A. A., and EL Gindy, A. A., 1988**. Storm surge generation by winter cyclones at Alexandria, Egypt, International Hydrographic Review, Monaco, pp. 129-139.
- **Howarth, P.J. and Wickmore, G.M. 1981,** Change detection in the Peace-Athabasca Delta using digital Landsat data, Remote Sensing of Environment, Vol. 11, pp. 9-25.
- **Mamdouh M. El-Hattab, 2015**, Improving Coastal Vulnerability Index of the Nile Delta Coastal Zone, Egypt. Journal of Earth Science & Climatic Change, Volume 6, Issue 8, 293, Elsevier.

- **Mamdouh M. El-Hattab, 2016**, Applying Post Classification Change Detection Technique to Monitor an Egyptian Coastal Zone (Abu Qir Bay). The Egyptian Journal of Remote Sensing and Space Sciences, Elsevier, 19, 23-36
- **Nelson, R.F. 1983**, Detecting forest canopy change due to insect activity using Landsat MSS. Photogrammetric Engineering and Remote Sensing, Vol. 49, pp. 1303-1314.
- **Robinove, C. J., P. J. Chavez, Gehring, O. and Holmgren, R. 1983**, Arid land monitoring using Landsat albedo difference images, Remote Sensing of Environment, Vol. 11, pp. 133-156.
- **Scott, T., 1954.** Sand movement by waves, US Army Corps Eng Beach Erosion Board, Tech. Memo., Vol. 48, pp. 37.
- **Sestini, G., 1991**. Implications of Climatic Changes for the Nile Delta, From L. Jeftic, J.D. Milliman, and G. Sestini (eds). Environmental and Social Impacts of Climate Change and Sea Level Rise in the Mediterranean Region, E. Arnold, London.
- **Smith, E. S., and Abdel-Kader, A., 1988**. Coastal erosion along the Egyptian Delta, Jour. of Coastal Research, U.S.A., Vol. 2, pp. 245-255.
- **Summerhayes, C.P., and Marks, N., 1976**. Nile Delta: Nature, Evolution, and Collapse of Continental Shelf Sediments: Proc. Sem. On Nile Delta Sed., UNDP/UNESCO/ASRT, pp. 28.
- **Susan R., F. Tempest, and T. Boyle, Sep. 1990**. The development and causes of range degradation features in southeast Botswana using multitemporal Landsat MSS imagery, Photogrammetric Engineering and Remote Sensing, Vol. 56, No. 9, pp. 1253-1262.
- **US Defense Mapping Agency 1961**, 1973, 1975, 1977.